Revised for *J. Geophys. Res.* 3 Feb 99

Stress Transfer by the 1988-89 M=5.3, 5.4 Lake Elsman Foreshocks to the Loma Prieta Fault: Unclamping at the Site of Peak Mainshock Slip

HUGO PERFETTINI

Laboratoire de Géologie, Ecole Normale Supérieure, Paris

ROSS S. STEIN and ROBERT W. SIMPSON

U.S. Geological Survey, Menlo Park

MASSIMO COCCO

Istituto Nazionale di Geofisica, Rome

Abstract. We study the stress transferred by the 27 June 1988 **M**=5.3 and 8 August 1989 **M**=5.4 Lake Elsman earthquakes, the largest events to strike within 15 km of the future Loma Prieta rupture zone during 74 years before the 1989 **M**=6.9 Loma Prieta earthquake. We find that the first Lake Elsman event brought the rupture plane of the second event 0.3-1.6 bars (0.03-0.16 MPa) closer to Coulomb failure, but that the Lake Elsman events did not bring the future Loma Prieta hypocentral zone closer to failure. Instead, the Lake Elsman earthquakes are calculated to have reduced the normal stress on (or 'unclamped') the Loma Prieta rupture surface by 0.5-1.0 bars (0.05-0.10 MPa) at the site where the greatest slip subsequently occurred in the Loma Prieta earthquake. This association between the sites of peak unclamping and slip suggests that the Lake Elsman events did indeed influence the Loma Prieta rupture process. Unclamping the fault would have locally lowered the resistance to sliding. Such an effect could have been enhanced if the lowered normal stress permitted fluid infusion into the unclamped part of the fault. Although less well recorded, the M_L=5.0 1964 and M_L=5.3 1967 Corralitos events struck within 10 km of the southwest end of the future Loma Prieta rupture. No similar relationship between the normal stress change and subsequent Loma Prieta slip is observed, although the high-slip patch southwest of the Loma Prieta epicenter corresponds roughly to the site of calculated Coulomb stress increase for a low coefficient of friction. The Lake Elsman-Loma Prieta result is similar to that for the 1987 **M**=6.2 Elmore Ranch-**M**=6.7 Superstition Hills earthquakes, suggesting that foreshocks might influence the distribution of mainshock slip rather than the site of mainshock nucleation.

INTRODUCTION

Several studies have identified the Lake Elsman earthquakes as rare events that struck within 5 km of the future Loma Prieta rupture plane, and only 11 km from the Loma Prieta hypocenter [Seeber and Armbruster, 1990; Olson, 1990; Olson and Hill, 1993] (Fig. 1). These authors argued that the lake Elsman events occurred on a steeply northeast-dipping oblique reverse fault, distinct from the Loma Prieta plane. Sykes and Jaumé [1990] regarded the Lake Elsman events as ‘long-term foreshocks’ to Loma Prieta, because of their proximity in space and time to the Loma Prieta rupture, and because they occurred on secondary faults, a feature they argue is typical of the seismic buildup to large events. After both

Lake Elsman earthquakes, the U.S. Geological Survey and California State Office of Emergency Services issued a joint advisory of a heightened probability of **M**=6.5 shocks during the succeeding 5 days. The advisory was partly motivated by the observation that the two Lake Elsman events were among the three largest shocks to occur anywhere along the extent of the 1906 San Andreas rupture since 1914. In addition, several studies had proposed that the section of the San Andreas adjacent to these events had a high probability of a large earthquake [see review by Harris, 1998].

Here we attempt to calculate the effect of the Lake Elsman shocks on the future Loma Prieta rupture. We seek answers to the question, Did the Lake Elsman events hasten the occurrence of the Loma Prieta shock, influence the site of its nucleation, or its distribution of earthquake slip?

OBSERVATIONS

Lake Elsman Earthquake Sequence

Although the aftershock sequences of the two Lake Elsman shocks are somewhat atypical for California events, little about them suggests that they would be the prelude to a nearby **M**=6.9 earthquake. Most aftershocks of the 27 June 1988 M_L=5.3 Lake Elsman event (hereinafter, *LE1*) clustered to the northwest of the mainshock, at the site of the subsequent 8 August 1989 M_L=5.4 Lake Elsman shock (hereinafter, *LE2*) (Fig. 2a). Aftershocks of the first event are unusually sparse, , and the aftershock decay rate is unusually slow (Fig. 2b), in relation to the California aftershock statistics of Reasenberg and Jones [1994]. The largest aftershock of *LE1* was just M_L=2.9. The aftershock decay rate is normal for *LE2* (Fig. 2b), but the ratio of large to small aftershocks is unusually high, including an M_L=4.3 30 min after the main shock, an M_L=4.5 shock after 7.7 hr, and an M_L=3.4 after 34 days (Fig. 2c). White and Ellsworth [1993] identified M_L=0.8 and M_L=1.2 shocks that occurred just 3.25 hr before the Loma Prieta main shock (Fig. 2c), both at the northwest end of the *LE2* aftershock zone. The precursory significance of these shocks is unknown.

Lake Elsman and Loma Prieta Source Parameters

The Lake Elsman events locate close to the junction of the San Andreas and Sargent faults on an unknown fault (or faults) with no surface trace. We use the focal mechanisms obtained for the Lake Elsman events by first motion polarities by Olson and Hill [1993], and locations and depths by joint hypocentral determination by Dietz and Ellsworth [1997] (Table 1). *LE1* struck at a depth of 13.2 km, 4 km from the future Loma Prieta rupture plane; *LE2* struck at a depth of 14.2 km, 5 km from the Loma Prieta plane. For both events one nodal plane strikes northwest and dips steeply northeast, aligned in map view with other earthquakes recorded during 1969-1989 (Fig. 1). Most faults in this region exhibit components of right-lateral and reverse slip, with the northeast side up [Seeber and Armbruster, 1990; Olson, 1990].

We developed source models for the nodal planes of each Lake Elsman event (Table 1), converting M_L to seismic moment M_o following Hanks and Kanamori [1979]. Although aftershocks of *LE2* extend over a 5-km-wide region, the rupture areas and hence static shear stress drops for these events are unknown. We thus set the stress drop equal to the regional mean value of ~25 bars (2.5 MPa) [Abercrombie, 1995]. The calculated stress changes presented in this study scale linearly with stress drop. To minimize stress discontinuities at the edges of the rupture surface, we prescribe slip on 3 nested planar squares centered at each hypocenter. For the northwest plane of *LE1*, the outer dimension of the slip surface is 3.8 km, for *LE2*, it is 4.25 km (Table 1).

The Loma Prieta earthquake occurred on 18 October 1989 GMT and nucleated at a depth of 15.9 km on a plane striking 128-130° and dipping 70° [Dietz and Ellsworth, 1997]. Its seismic moment is 2.2-3.2 x 10^{19} N-m (M_W=6.9), the mean static stress drop is about 35 bars (3.5 MPa), slip was confined to a depth of 7-20 km and extended about 35 km along strike [see review by Spudich, 1996].

MODELING

We calculate the normal and shear stress changes resolved onto the second Lake Elsman earthquake by the first, and by both Lake Elsman earthquakes on the Loma Prieta slip surface, using Robert Simpson's program, DLC [Reasenberg and

Simpson, 1992; Simpson and Reasenberg, 1994]. The Coulomb failure stress change (*ΔCFF*) can be written

$$\Delta CFF = \Delta\tau + \mu\ (\Delta\sigma_n - \Delta P) \qquad (1)$$

where $\Delta\tau$ the change in shear stress in the rake direction, μ is the static friction coefficient, $\Delta\sigma_n$ the change in normal stress, and ΔP is the change in pore pressure.

We interpret a positive value of *ΔCFF* to mean that a fault patch has been brought closer to failure; when *ΔCFF* is negative, the fault is brought further from failure. We calculate only the change in stress, without reference to how close a fault was to failure beforehand. Thus, no information is needed or assumed about the regional or absolute stress field. We investigate end-member friction coefficients, μ, of 0.8, a value for unsaturated rocks obeying Byerlee's law; and 0.0, a value appropriate if the Loma Prieta fault were frictionally weak, as suggested by Beroza and Zoback [1993] and Zoback and Beroza [1993]. Calculations are made in a uniform elastic halfspace with a Poisson's ratio, ν, of 0.25, and the shear-modulus of 30 GPa (3×10^{11} dyne-cm^{-2}). More complete discussions of the Coulomb stress change can be found in Simpson and Reasenberg [1994] and King et al [1994].

To calculate the stress transferred by the Lake Elsman events onto the Loma Prieta fault, we utilize information on the distribution of Loma Prieta earthquake slip and rake. First, we resolve the normal stress change caused by the Lake Elsman events on each sub-patch of the Loma Prieta fault. Next we resolve the shear stress change on each sub-patch for the modeled slip rake of that patch. We consider two planar models of variable slip on the fault plane, Beroza [1996] and Wald et al [1996] (earlier versions of these models appeared as Beroza [1991] and Wald et al [1991]). In these models both the rake and slip magnitude vary from one sub-patch to the next. Beroza [1996] used high-frequency strong-motion data to invert for the fault slip, dividing the fault into 41 along-strike by 7 down-dip patches, for 287 sources. His rupture plane strikes 130°, dips 70°, and extends over a depth of 5-18 km. Wald et al [1996] inverted high frequency strong-motion data and broadband teleseismic data on 12 along-strike by 8 down-dip patches, for 96 sources. His plane strikes 128°, dips 70°, and extends over a depth of 1.5-20.3 km. We focus our analysis on the common features of these fault-slip models, which, along with nearly all other inversions for the earthquake slip, display two isolated zones of high slip, northwest and southeast of the hypocenter (see Guatteri and Cocco [1996], and references therein).

RESULTS

Promotion of the second Lake Elsman earthquake by the first

We find that the second event, *LE2*, was brought closer to Coulomb failure by the first, *LE1* (Fig. 3 and Table 2). Because of the roughly symmetrical four-lobed pattern of stress-change, *LE1* would promote failure on *LE2* regardless of which nodal plane is assumed. The stress increase is largest (1.6 bars or 0.16 MPa for μ=0.4) if both rupture planes strike northwest, as suggested by Seeber and Armbruster [1990], Olson [1990], and Olson and Hill [1993]. It is evident from Fig. 3 that the *LE2* plane is optimally located for stress transfer from *LE1*, and also that this result is insensitive to the assumed friction coefficient. Most aftershocks of *LE1* occur in the vicinity of the future *LE2* site to the northwest of *LE1* (Fig. 2a). The calculated stress transfer for all four nodal-plane combinations is listed in Table 2.

Stress Transferred by the Lake Elsman shocks to the Loma Prieta fault

The top three panels of Fig. 4 show the normal, right-lateral, and reverse components of the stress transferred by the Lake Elsman events on to the Loma Prieta rupture surface. Our sign convention is that unclamping and a shear stress increase in the rake direction, are positive (red), promoting failure. We resolve the Coulomb stress change using the rake on each patch furnished by Beroza [1996] in the bottom panel of Fig. 4. Stress changes induced by the Lake Elsman shocks are resolved on to the rupture plane of Wald et al [1996] in Fig. 5. The Loma Prieta slip vectors are shown in the top and bottom panels of both figures. Slip vectors for patches with slip greater than 1 m are shown, but the vectors for all sources are used in the calculations. Beroza [1996] and Wald et al [1996] both find high slip sites northwest and southeast of the hypocenter. The principal difference between the two slip models, and the resulting Coulomb stress change, is that in the site northwest of the Loma Prieta epicenter, Beroza [1996] finds nearly pure reverse slip and Wald et al [1996] find oblique right-lateral slip.

The most striking observation is that the Lake Elsman events unclamped the Loma Prieta fault where it subsequently slipped the most (compare the top panels of Figs. 4 and 5; unclamping is red and clamping is blue), as previously reported by Llewellin and Ellis [1994]. The calculated normal stress change at the site of greatest slip northwest of the hypocenter is apparent in both Beroza [1996] and Wald et al [1996] models. The peak unclamping on the Loma Prieta fault is 1.10 bars (0.11 MPa) at a depth of 12-13 km; the average normal stress change over the entire high-slip patch is 0.45 bars (0.45 MPa) in the Beroza [1996] model. It is 0.75 bars (0.075 MPa) in the Wald et al [1996] model, because the site of high slip is more restricted. This result is insensitive to the nodal planes assumed to have slipped in the Lake Elsman earthquakes. The normal stress change is shown for all four nodal-plane combinations in Fig. 6; the site of unclamping corresponds to the high slip in each case. The correlation is also insensitive to the precise depth and location of the Lake Elsman sources, and the strike and location of the Loma Prieta rupture surface. This is illustrated in Fig. 7, a horizontal slice at the depth of the Lake Elsman earthquakes: Neither the magnitude nor the along-strike extent of the unclamped site would vary significantly if the relative locations were in error by ≤ 1.5 km.

The unclamping corresponds more closely to the site of peak Loma Prieta slip than does the Coulomb stress increase. The Coulomb stress change for a high coefficient of apparent friction is shown in the bottom panels of Fig. 4 and Fig. 5.

For $\mu = 0.8$, the peak Coulomb stress increase is 0.80 bars (0.08 MPa); the average increase is 0.20 bars (0.02 MPa) in the Beroza model and 0.25 bars (0.025 MPa) in the Wald et al model. For $\mu = 0.0$, the peak increase is 0.50 bars (0.05 MPa), but this occurs beneath the site of high slip, and the average Coulomb stress change over the high-slip site is slightly negative.

There is no association between the rake of the applied shear stress change and the rake of the fault slip, northwest of the hypocenter. For example, the site of reverse slip northwest of the Loma Prieta epicenter does not correspond to reverse shear-stress increase associated with the Lake Elsman (Fig. 4 and Fig. 5). This is consistent with the view advanced by others that the fault rake is governed by the total shear stress during slip, a product of the total static stress and the dynamic stress during rupture [Guatteri and Cocco, 1996]. The static stress is more likely to be the product of permanent fault features, such as its local strike and dip. Indeed, the bend in the strike of the San Andreas fault near the Loma Prieta mainshock requires a reverse component of slip and a non-vertical dip northwest of the epicenter [Anderson, 1990], consistent with the observed rake variation.

Stress transferred by the Lake Elsman shocks to the Loma Prieta hypocenter

The Lake Elsman earthquakes did not bring the Loma Prieta fault closer to Coulomb failure at the future hypocenter. This result is inescapable, because the Coulomb stress change is negative regardless of the apparent friction coefficient, the assumed Lake Elsman nodal planes, or the hypocentral rake (Fig. 4 and Fig. 5). Although the Loma Prieta hypocenter is unclamped by 0.05-0.10 bars (0.005-0.010 MPa), the right-lateral and reverse shear stress changes are slightly negative,-0.10 to -0.15 bars), inhibiting failure. Thus these calculations suggest that the seismic initiation of rupture was neither triggered nor directly promoted by the Lake Elsman events.

Stress transferred by 1964-1967 Corralitos shocks to the Loma Prieta fault

The correspondence between the site of calculated unclamping and the zone of high slip northwest of the Loma Prieta epicenter invites inquiry into whether a similar process could explain the high-slip patch southeast of the Loma Prieta epicenter. Three $M_L \geq 5.0$ earthquakes took place 22-26 years before the Loma Prieta event: the 14 September 1963 $M_L = 5.4$ Salinas-Watsonville event, and the 16 November 1963 $M_L = 5.0$ and 18 December 1967 $M_L = 5.3$ Corralitos events (Fig. 1 and Table 3). Focal mechanisms and locations are reported in Udias [1965], McEvilly [1966], Bolt et al [1968], Bolt and Miller [1971], and Wesson and Ellsworth [1973]; here we use relocations by Dietz and Ellsworth [1997]. The 1963 shock was located 13 km from the southeast end of the Loma Prieta rupture, 30 km from the Loma Prieta mainshock, too far to have transferred significant stress. The Corralitos events locate 4.5 km apart (Fig. 1), and share similar focal mechanisms; of these, the larger 1967 shock is best constrained due to seismic network enhancement after 1966. We assigned the 154° rake of the 1967 event and a shear stress drop of 30 bars to both shocks. Because of the character of nearby faults, pure right-lateral slip was also tried for the 1964 event, but the difference in stress transfer was negligible.

Although the source parameters of the Corralitos events are more uncertain than those of the Lake Elsman shocks, the 1964-67 events do not appear to have unclamped the high-slip zone southeast of the Loma Prieta earthquake (Fig. 8, top panel). Instead, the Corralitos events are calculated to have unclamped the Loma Prieta fault from the surface to a depth of about 12 km, whereas the high-slip zone lies at a depth of 9-18 km at approximately the same location along strike. The Coulomb stress change for a near-zero friction coefficient exhibits a weak correlation with the site of peak Loma Prieta slip (Fig. 8, middle panel). The long-term tectonic loading of about 0.1 bar/yr during the 22 years between 1967 and 1989, would augment the shear stress by ~2 bars (0.2 MPa), however, much larger than the ~0.3 bar (0.03 MPa) changes associated with the Corralitos events, presumably diminishing their effect. In sum, uncertainty on the location, depth, focal mechanisms, and size of the Corralitos events makes inferences about the role of the 1964-67 shocks quite frail, but based on available data, they do not appear to have unclamped the adjacent high-slip patch of the Loma Prieta shock.

OTHER EXAMPLES OF UNCLAMPING AT THE SITE OF PEAK SLIP

Corroborating evidence for the Lake Elsman-Loma Prieta findings is seen in the 1987 Elmore Ranch-Superstition Hills sequence. The 23 November **M**=6.2 left-lateral Elmore Ranch rupture was followed 11 hr later by a conjugate **M**=6.6 rupture on the Superstition Hills fault. The Elmore Ranch mainshock lies 10 km from the Superstition Hills mainshock. Hudnut et al [1989] used a 2-D elastic model to show that the epicentral end of the Superstition Hills fault was strongly unclamped by the Elmore Ranch shock. The region of peak slip was unclamped by about 30 bars (3.0 MPa). The shear stress change along the Superstition Hills fault is negative at the high slip patch, and so would not promote failure at the epicentral end of the rupture. Subsequently published variable slip models for the Superstition Hill earthquake using strong motion data [Wald et al, 1990] and GPS data [Larsen, 1992] reveal that the peak slip on the Superstition Hill fault occurred at or near the site of greatest unclamping associated with the preceding Elmore Ranch event. Thus in a case with roughly comparable earthquake magnitudes and distances (but a much shorter time scale, and which does not suffer from the uncertainties of the Corralitos events, a relationship similar to Lake Elsman-Loma Prieta events is evident.

INTERPRETATION

Here we offer several tentative explanations for the correlation between the unclamped area and the site of high Loma Prieta slip northwest of the epicenter. Since the second Lake Elsman event contributes most of the calculated normal stress change, the >70-day delay before the Loma Prieta rupture also merits consideration. The response of a fault to a sudden drop in normal stress, as simulated in laboratory experiments by Byerlee [1978], Linker and Dieterich [1992], and Anooshehpoor and Brune [1994], is a reduction of fault friction, which reduces resistance to sliding. Such a reduced value of fault friction might permit locally higher slip. It would, however, seem remarkable that a 1-bar (0.1 MPa) drop in normal stress could cause the observed 2-3 fold increase in fault slip; the shear stress drop in the high-slip zone, for example, is ~130-220 bars (13-22 MPa) [Wald et al, 1994]. But in the rate and state formulation of Linker and Dieterich [1992], a very small normal stress change relative to the total normal stress, causes a large and sudden drop in sliding resistance that can further amplify the sudden change. This phenomenon is observed in laboratory experiments with samples of numerous rock types, and does not require the presence of fluids. Because the Loma Prieta earthquake was not immediately triggered by either of Lake Elsman events, the drop in normal stress may not have been sufficient to cause earthquake nucleation, or the normal stress reduction occurred on a part of the fault that was not near the failure threshold.

It is also possible that the Lake Elsman earthquakes could have indirectly triggered the Loma Prieta earthquake: The Loma Prieta hypocenter lies on the southern edge of the unclamped zone (see the top panel of Fig. 4). If the unclamped zone underwent creep during the 70-480 days preceding the Loma Prieta mainshock, then the periphery of the creep zone would have sustained a shear stress increase. The hypocenter lies along this periphery. No continuous strain instruments were located close to the Lake Elsman or Loma Prieta epicenters. Nevertheless, preseismic slip was not reliably detected by geodetic [Lisowski et al, 1993] or continuous strain [Johnston and Linde, 1993] observations, and so we can offer no direct support for this hypothesis.

Pore fluid flow into the part of the fault unclamped by the Lake Elsman events provides another mechanism that might explain both the large increase in Loma Prieta slip and the time delay. . With continued ductile creep or tectonic loading during the intervening 70-480 day period, the pore pressure in the unclamped zone might rise to a level similar to the surrounding parts of the fault. Such a fluid-enriched zone might offer a lower resistance to sliding when the rupture front passed through during the Loma Prieta event. Sleep and Blanpied [1992] and Blanpied et al [1992] have argued that interseismic ductile creep compacts the fault zone and occurs at stresses far below those needed for frictional failure. Fault compaction would raise the fluid pressure, enabling frictional failure at relatively low shear stress [Rice, 1992]. The limitation on such hypotheses is that we have no direct evidence for such preseismic fluid flow.

An interpretation independent of our stress calculations is that the total shear stress was highest in the vicinity of the Lake Elsman shocks and the future site of high slip in the Loma Prieta event. Because the total stress state and its spatial variation is unknown, this speculation is difficult to test. The strongest argument in its favor is the proximity of *LE1* to the high slip patch. In contrast, the larger *LE2* and its principal aftershocks lie well to the north of the high slip patch (top panel of Fig. 4). A similar argument could be advanced that the association of the southeast slip patch and the Corralitos events suggests this region, too, sustained a higher total stress. The Corralitos shocks appear, however, to be considerably shallower than the site of high Loma Prieta slip (Fig. 8).

CONCLUSION

Neither the 1988-89 Lake Elsman nor the 1964-67 Corralitos earthquakes increased the Coulomb stress at the future Loma Prieta hypocenter, and thus it is unlikely that these events hastened the occurrence of the Loma Prieta earthquake.. This finding is in accord with the study by Dodge et al [1996], who examined six California foreshock sequences and also found no tendency for the future hypocentral site to be brought closer to Coulomb failure, or to be unclamped, by the foreshocks. Instead, we suggest that the Lake Elsman events are more likely to have influenced the distribution of slip on the Loma Prieta fault. This inference is predicated on the association between the patch of high slip northwest of the Loma Prieta epicenter and the site where we calculate the Lake Elsman earthquakes to have unclamped the fault. A correlation between the zone of high slip and the Coulomb stress change for a high apparent coefficient of friction is also evident, though not as persuasive. A reduction in normal stress on part of the Loma Prieta fault could have increased the subsequent slip by lowering the fault friction, or by permitting infiltration of pore fluids. The 1987 Elmore Ranch-Superstition Hills earthquakes suggest a similar pattern, a large foreshock unclamping the site of greatest slip on the mainshock. If it were demonstrated by further studies that small shocks occurring late in the earthquake cycle affect the subsequent distribution of slip, then the role of foreshocks would be seen in a new light. Such a demonstration would also call into question the hypothesis of characteristic earthquake slip, in which faults produce similar slip distributions in successive earthquakes.

Acknowledgements. We thank Jean Schmittbuhl, Raul Madariaga, and Olivier Ronsin for many essential discussions, Steve Walter and Lynn Dietz for their seismicity maps, and David Wald, Bill Ellsworth, Ruth Harris, Greg Beroza, Doug Dodge and an anonymous referee for thoughtful reviews. This study was funded by the Pacific Gas & Electric Co. through a cooperative research and development agreement with the USGS.

REFERENCES

Abercrombie, R. E., Earthquake source scaling relationships from –1 to 5 M_L using seismograms recorded at 2.5-km depth, *J. Geophys. Res.*, **100**, 24,015-24,036, 1995.

Anderson, R. S., Evolution of the northern Santa Cruz Mountains by advection of crust past a San Andreas fault bend, *Science*, **249**, 397-401, 1990.

Anooshehpoor, A. and J.N. Brune, Frictional heat generation and seismic radiation in a foam rubber model of earthquakes, *Pageoph*, **142**, 735-747, 1994.

Beroza, G. C., Near-source modeling of the Loma Prieta earthquake: evidence for heterogeneous slip and implications for earthquake hazard, *Bull. Seismol. Soc. Amer.*, **81**, 1603-1621, 1991.

Beroza, G. C., Rupture history of the earthquake from high-frequency strong-motion data, in P. Spudich (Ed.), The Loma Prieta, California, Earthquake of October 17, 1989—Main-Shock Characteristics, *U.S. Geol. Surv. Prof. Pap. 1550-A*, 9-32, 1996.

Beroza, G.C., and M.D. Zoback, Mechanism diversity of the Loma Prieta aftershocks and the mechanics of mainshock-aftershock interaction, *Science*, **259**, 210-213, 1993.

Blanpied, M.L., D.A. Lockner, and J.D. Byerlee, An earthquake mechanism based on rapid sealing of faults, *Nature*, **358**, 574-576, 1992.

Bolt, B.A., C. Lomnitz, and T.V. McEvilly, Seismological evidence of the tectonics of Central and Northern California and the Mendocino escarpment, *Bull. Seismol. Soc. Amer.*, **58,** 1725-1767, 1968.

Bolt, B.A., and R.D. Miller, Seismicity of Northern and Central California, 1965-1969, *Bull. Seismol. Soc. Amer.*, **61**, 1831-1847, 1971.

Byerlee, J.D., Friction of rock, *Pageoph*, **116**, 615-626, 1978.

Dietz, L.D. and W.L. Ellsworth, Aftershocks of the 1989 Loma Prieta earthquake and their tectonic implications, in Reasenberg, P.A. (Ed.), The Loma Prieta, California, earthquake of October 17, 1989—Aftershocks and postseismic effects, *U. S. Geol. Surv. Prof. Pap. 1550-D,* 5-48, 1997.

Dodge, D.A., G.C. Beroza, and W.L. Ellsworth, Detailed observations of California foreshock sequences: Implications for the earthquake initiation process, *J. Geophys. Res*., **101**, 22,371-22,392, 1996.

Gomberg, J., N. Beeler, M. Blanpied, and P. Bodin, Earthquake triggering by transient and static deformation, *J. Geophys. Res.,*, in press, 1998.

Guatteri, M., and M. Cocco, On the variation of slip direction during the earthquake rupture: Supporting and conflicting evidence from the 1989 Loma Prieta earthquake, *Bull. Seismol. Soc. Amer*., **86**, 1935-1951, 1996.

Hanks T.C, and H. Kanamori, A moment magnitude scale, *J. Geophys. Res,* **84**, 2348-2350, 1979.

Harris R.A., The Loma Prieta, California, Earthquake of October 17, 1989— Forecasts, *U.S. Geol. Surv. Prof. Pap. 1550-B*, 3-28, 1998.

Hudnut, K.W., L. Seeber, and J. Pacheco, Cross-fault triggering in the November 1987 Superstition Hills earthquake sequence, southern California, *Geophys. Res. Lett*., **16**, 199-202, 1989.

Johnston, M.J.S., and A.T. Linde, Near-field high-resolution strain measurements, in M.J.S. Johnston, (Ed.), The Loma Prieta, California, earthquake of October 17, 1989—Preseismic Observations, *U.S. Geol. Surv. Prof. Pap. 1550-C*, 53-58, 1993.

King G.C.P., R.S. Stein, and J. Lin, Static Stress Changes and the Triggering of Earthquakes, *Bull. Seismol. Soc. Amer*, **84**, 935-953, 1994.

Larsen, S., R. Reilinger, H. Neugebauer, and W. Strange, Global Positioning System measurements of deformation associated with the 1987 Superstition Hills earthquake: Evidence for conjugate faulting, *J. Geophys. Res,* **97**, 4885-4902, 1992.

Linker, M.F., and J.H. Dieterich, Effects of variable normal stress on rock friction: Observations and constitutive equations, *J. Geophys. Res*., **97**, 4923-4949, 1992.

Lisowski, M., J.C. Savage, W.H. Prescott, J.L. Svarc, and M.H. Murray, No convincing precursory geodetic anomoly observed, in M.J.S. Johnston, (Ed.), The Loma Prieta, California, earthquake of October 17, 1989—Preseismic Observations, *U.S. Geol. Surv. Prof. Pap. 1550-C*, 67-72, 1993.

Llewellin, M., and M.A. Ellis, Generation of the northwestern asperity in the 1989 Loma Prieta rupture, *EOS, Trans. Amer. Geophys. Un.*, **76**, Fall Mtg. Suppl., 575, 1994.

McEvilly T.V, The earthquake sequence of November 1964 near Corralitos Nevada, *Bull. Seismol. Soc. Amer*, **56,** 755-773, 1966.

Olson, J.A., Seismicity in the twenty years preceding the Loma Prieta, California earthquake, *Geophys. Res. Lett.* , **17**, 1429-1432, 1990.

Olson, J.A. and D.P. Hill, Seismicity in the southern Santa Cruz Mountains during the 20-year period before the earthquake, in M.J.S. Johnston, Ed., The Loma Prieta, California, earthquake of October 17, 1989—Preseismic observations, *U.S. Geol. Surv. Prof. Pap. 1550-C*, 3-16, 1993.

Reasenberg, P.A., and R.W. Simpson, Response of Regional Seismicity to the Static Stress Change Produced by the Loma Prieta Earthquake, *Science*, **255**, 1687-1690, 1992.

Reasenberg, P.A., and L.M. Jones, Earthquake aftershocks: Update, *Science*, **265**, 1251-1252, 1994.

Rice, J.R., Fault stress states, pore pressure distributions, and the weakness of the San Andreas fault, in B. Evans and T.-F. Wong (Eds.), *Fault Mechanics and Transport Properties of Rocks*, pp. 475-503, Academic Press, San Diego, 1992.

Scholz, C.H., *The Mechanics of Earthquakes and Faulting,* Cambridge Univ. Press, Cambridge, 439 p., 1990.

Seeber, L. and J.G. Armbruster, Fault kinematics in the 1989 Loma Prieta rupture area during 20 years before that event, *Geophys. Res. Lett.*, **17**, 1425-1428, 1990.

Simpson, R.W., and P.A. Reasenberg, Earthquake-Induced Static-Stress Changes on Central California Faults, The Loma Prieta, California, Earthquake of October 17, 1989—Tectonic Processes and Models, *U.S. Geol. Surv. Prof. Pap. 1550-F*, 55-89, 1994.

Sleep, N.H and M.L. Blanpied, Creep, compaction and the weak rheology of major faults, *Nature*, **359**, 687-692, 1992.

Spudich, P., Synopsis, in P. Spudich (Ed.), The Loma Prieta, California, Earthquake of October 17, 1989—Main-Shock Characteristics, *U.S. Geol. Surv. Prof. Pap. 1550-A*, 1-7, 1996.

Sykes, L.R., and S.C. Jaumé, Seismic activity on neighboring faults as a long-term precursor to large earthquakes in the San Francisco Bay area, *Nature*, **348**, 595-599, 1990.

Udias, A.S.J., A study of the aftershocks and focal mechanism of the Salinas-Watsonville earthquakes of August 31 and September 14, 1963 *Bull. Seismol. Soc. Amer*,, **55**, 85-106, 1965.

Wald, D.J., D.V. Helmberger, and S.H. Hartzell, Rupture process of the 1987 Superstition Hills earthquake from the inversion of strong motion data, *Bull. Seismol. Soc. Amer.*, **80**, 1079-1098, 1990.

Wald, D.J., D.V. Helmberger, and T.H. Heaton, Rupture model of the 1989 Loma Prieta earthquake from inversion of strong-ground motion and broadband teleseismic data, *Bull. Seismol. Soc. Amer.*, **81**, 1540-1572, 1991.

Wald, D.J., D.V. Helmberger, and T.H. Heaton, Strong-motion and broadband teleseismic analysis of the earthquake for rupture-process modeling and hazard assessment, in P. Spudich (Ed.), The Loma Prieta, California, Earthquake of October 17. 1989—Main-shock characteristics, *U.S. Geol. Surv. Prof. Pap. 1550-A*, 235-262, 1996.

Walter, S.R., D.H. Oppenheimer, and R.I. Mandel, Seismicity map of the San Francisco-San Jose 1:250,000 quadrangle, California, for the period 1967-1993, *U.S. Geol. Surv. Geol. Investiga. Series, Map I-2580* (3 sheets), 1998.

Wesson, R.L, and W.L. Ellsworth, Seismicity preceding moderate earthquake in California, *J. Geophys. Res,* **78**, 8527-8546, 1973.

White, R.A., and W.L. Ellsworth, Near-source short- to intermediate-period ground motions, in M.J.S. Johnston (Ed.), The Loma Prieta, California, earthquake of October 17, 1989—Preseismic observations, *U.S. Geol. Surv. Prof. Pap. 1550-C*, 31-46, 1993.

Zoback, M.D., and G.C. Beroza, Evidence for near-frictionless faulting in the 1989 (M 6.9) Loma Prieta, California, earthquake and its aftershocks, *Geology*, **21**, 181-185, 1993.

FIGURE CAPTIONS

Fig. 1. Seismicity of the Loma Prieta area (1/1/67-1/1/93) modified from Walter et al [1998]. The map (*lower panel*) displays earthquakes within 5 km of the slip plane. Seismicity plotted in the along-strike (*A-A′*) and across-strike (*B-B′*) depth sections is bounded by the dashed lines on the map. The parallelograms in *A-A′* and *B-B′* are the outer slip surfaces of the northwest-striking nodal planes used to model the Lake Elsman earthquakes..

Fig. 2. Aftershocks of the Lake Elsman earthquakes. (***a***) Map of *LE1* (6/27/88-8/8/89) and *LE2* (8/8/89-10/17/89) aftershocks. (***b***). Aftershock decay rate. (***c***) Earthquake magnitude as a function of time for *LE2*.

Fig. 3. Map view of the Coulomb stress change associated with the 27 June 1988 Lake Elsman earthquake (*LE1*) for friction coefficients, μ=0.0 and μ=0.8. Stress is calculated at the depth of *LE2*, 14 km; (0,0) km corresponds to 122.0°W/37.0°N. The nested rectangles are the modeled slip surfaces. The red dashed line identifies the intersection of the Loma Prieta slip plane of Beroza [1996].

Fig. 4. Stress change associated with the *LE1* and *LE2* earthquakes resolved onto the Beroza [1996] slip plane of the Loma Prieta earthquake, under the assumption that both *LE* ruptures strike northwest. Note that the color bar saturates at ±0.5 bars, although that the stress changes exceed this value. The green (*LE1*) and magenta (*LE2*) parallelograms depict the perimeters of the Lake Elsman source models. Loma Prieta slip vectors for those patches in which the

net slip exceeds 1.5 m are plotted as vectors in the top and bottom panels. The grid spacing of Beroza used in our calculations is indicated by the rectangles in the corners of the Loma Prieta slip plane. The first 1,000 hr of aftershocks are plotted with shocks lightening with time in the sequence.

Fig. 5. Same as Fig. 4, except that stress changes are resolved on the Wald et al [1996] Loma Prieta slip model. The grid spacing of Wald et al used in our calculations is indicated by the rectangles in the corners of the Loma Prieta slip plane.

Fig. 6. The normal stress change associated with the Lake Elsman earthquakes resolved on the Beroza et al [1996] slip surface, under the four possible nodal plane scenarios. '*1=NE, 2=NW*' designates the northeast-striking nodal plane for *LE1* and the northwest-striking plane for *LE2*, etc.

Fig. 7. Map view of the normal stress changes associated with the Lake Elsman earthquakes calculated at a depth of 13 km (their average depth), resolved onto planes parallel to the Loma Prieta slip surface of Beroza [1996]. The Loma Prieta surface intersects the calculation depth at the yellow dashed line.

Fig. 8. The normal and Coulomb stress changes associated with the 16 November 1964 M_L=5.0 and 18 December 1967 M_L=5.3 Corralitos earthquakes, resolved onto the Beroza [1996] plane under the assumption that slip occurred on the northwest-striking nodal planes. The outer edge of the

modeled 1964 and 1967 slip surfaces are the green and magenta lines, respectively.

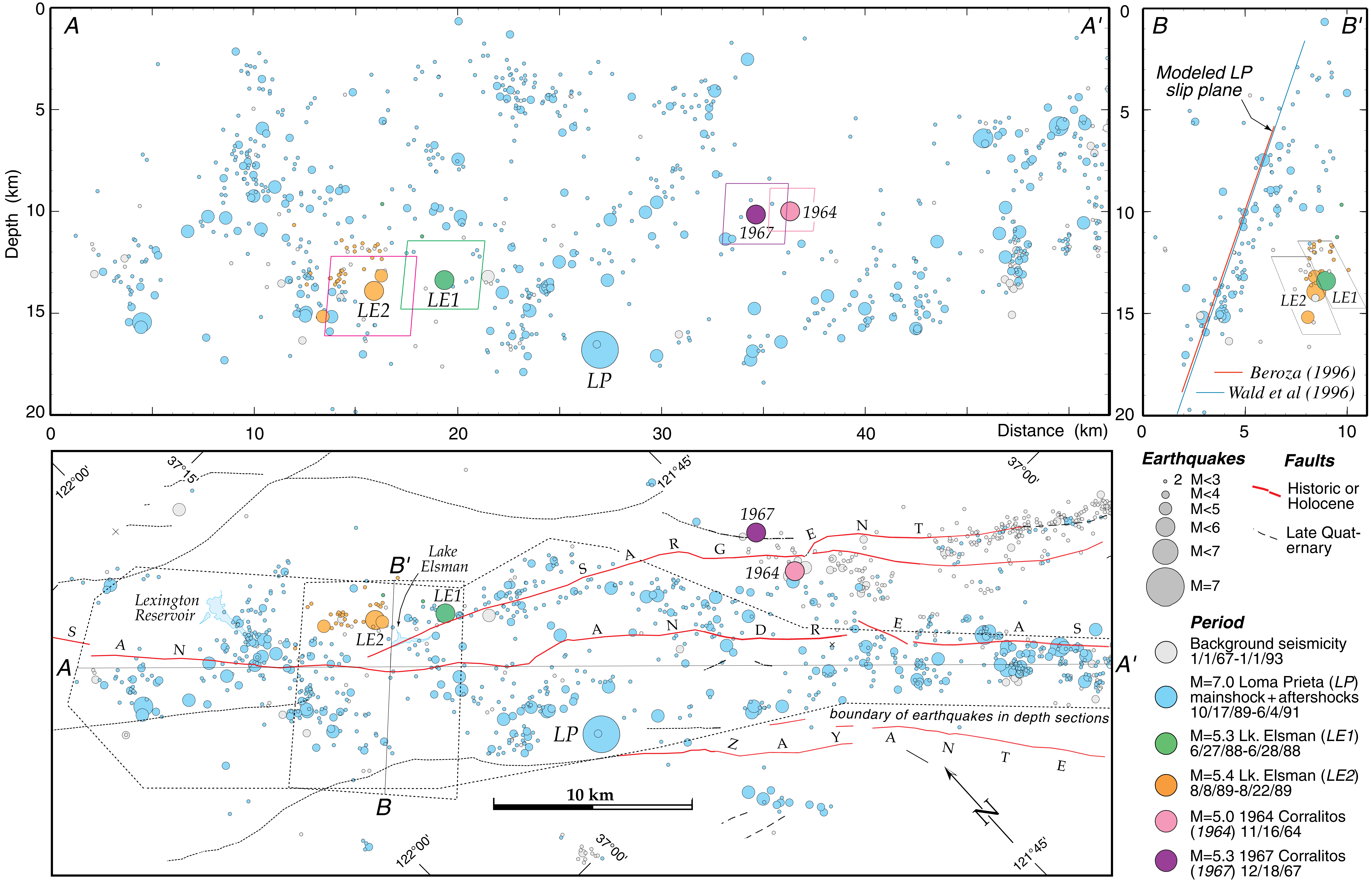

A
A'
B
B'
Depth (km)
0
5
10
15
20
Distance (km)
0
10
20
30
40
LE2
LE1
LP
1967
1964
Modeled LP slip plane
Beroza (1996)
Wald et al (1996)
122°00'
37°15'
121°45'
37°00'
Lexington Reservoir
Lake Elsman
S A N
S A R G E N T
A N D R E A S
Z A Y A N T E
boundary of earthquakes in depth sections
10 km
N
Earthquakes
2 M<3
M<4
M<5
M<6
M<7
M=7
Faults
Historic or Holocene
Late Quaternary
Period
Background seismicity 1/1/67-1/1/93
M=7.0 Loma Prieta (LP) mainshock+aftershocks 10/17/89-6/4/91
M=5.3 Lk. Elsman (LE1) 6/27/88-6/28/88
M=5.4 Lk. Elsman (LE2) 8/8/89-8/22/89
M=5.0 1964 Corralitos (1964) 11/16/64
M=5.3 1967 Corralitos (1967) 12/18/67

Fig. 1 *1 Feb 99*

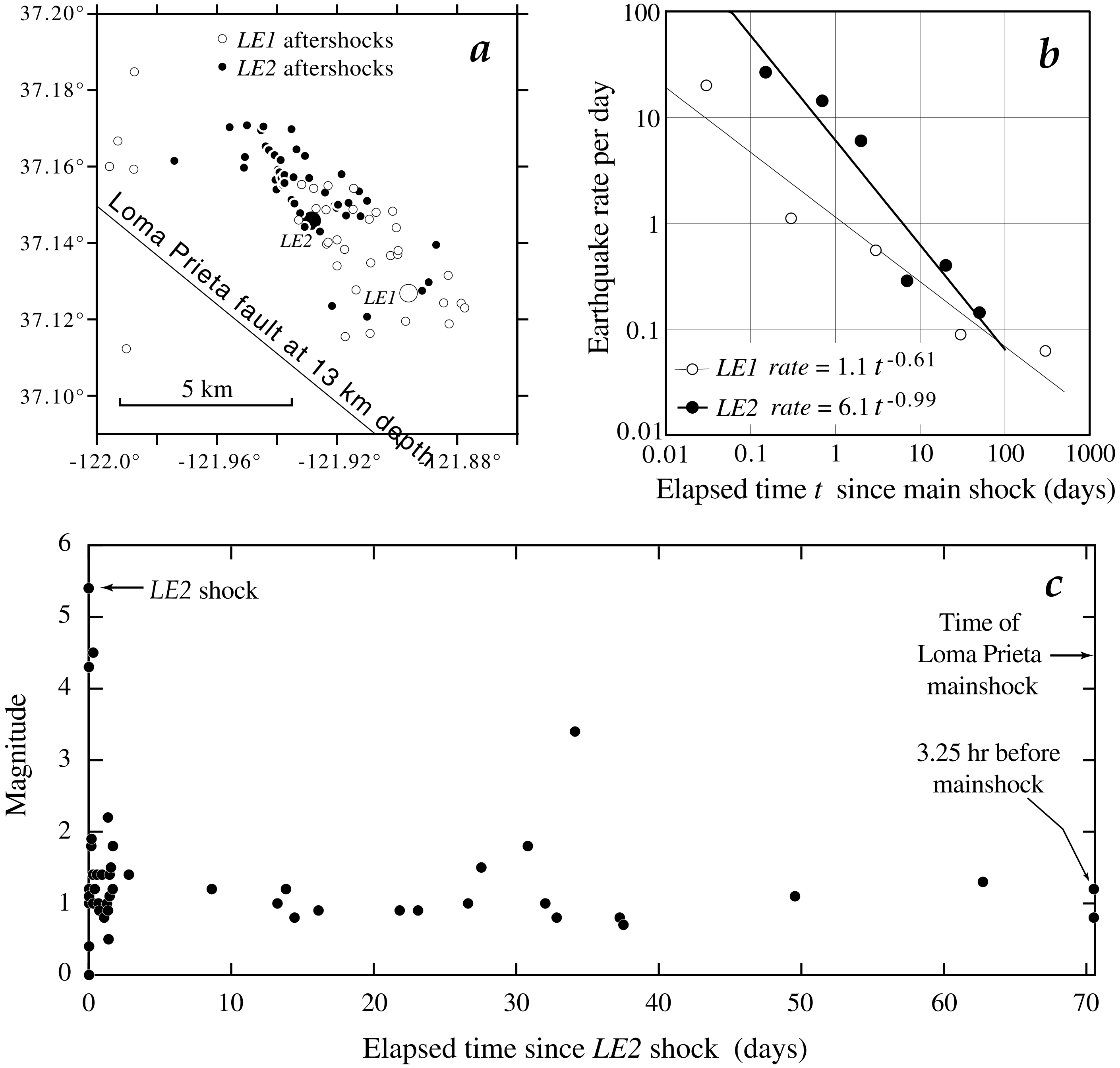
37.20°
37.18°
37.16°
37.14°
37.12°
37.10°
-122.0°
-121.96°
-121.92°
-121.88°
LE1 aftershocks
LE2 aftershocks
a
LE2
LE1
Loma Prieta fault at 13 km depth
5 km
b
100
10
1
0.1
0.01
0.01
0.1
1
10
100
1000
Earthquake rate per day
Elapsed time t since main shock (days)
LE1 rate = 1.1 t^-0.61
LE2 rate = 6.1 t^-0.99
c
6
5
4
3
2
1
0
Magnitude
LE2 shock
Time of
Loma Prieta
mainshock
3.25 hr before
mainshock
0
10
20
30
40
50
60
70
Elapsed time since LE2 shock (days)

Fig. 2 *1 Feb 99*

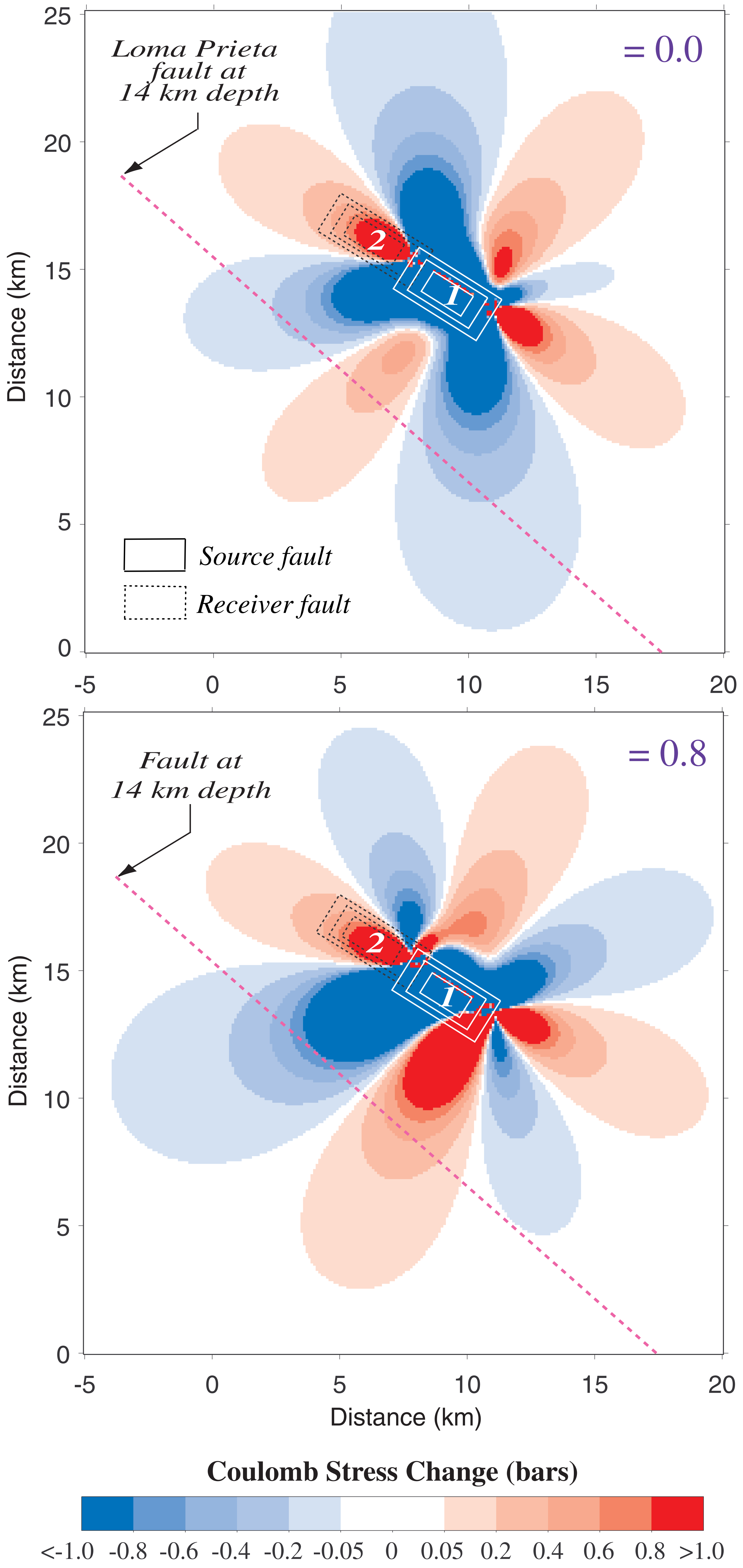
Loma Prieta
fault at
14 km depth
= 0.0
2
1
Source fault
Receiver fault
Fault at
14 km depth
= 0.8
Distance (km)
Distance (km)
25
20
15
10
5
0
-5
0
5
10
15
20
Coulomb Stress Change (bars)
<-1.0
-0.8
-0.6
-0.4
-0.2
-0.05
0
0.05
0.2
0.4
0.6
0.8
>1.0

Fig. 3 *1 Feb 99*

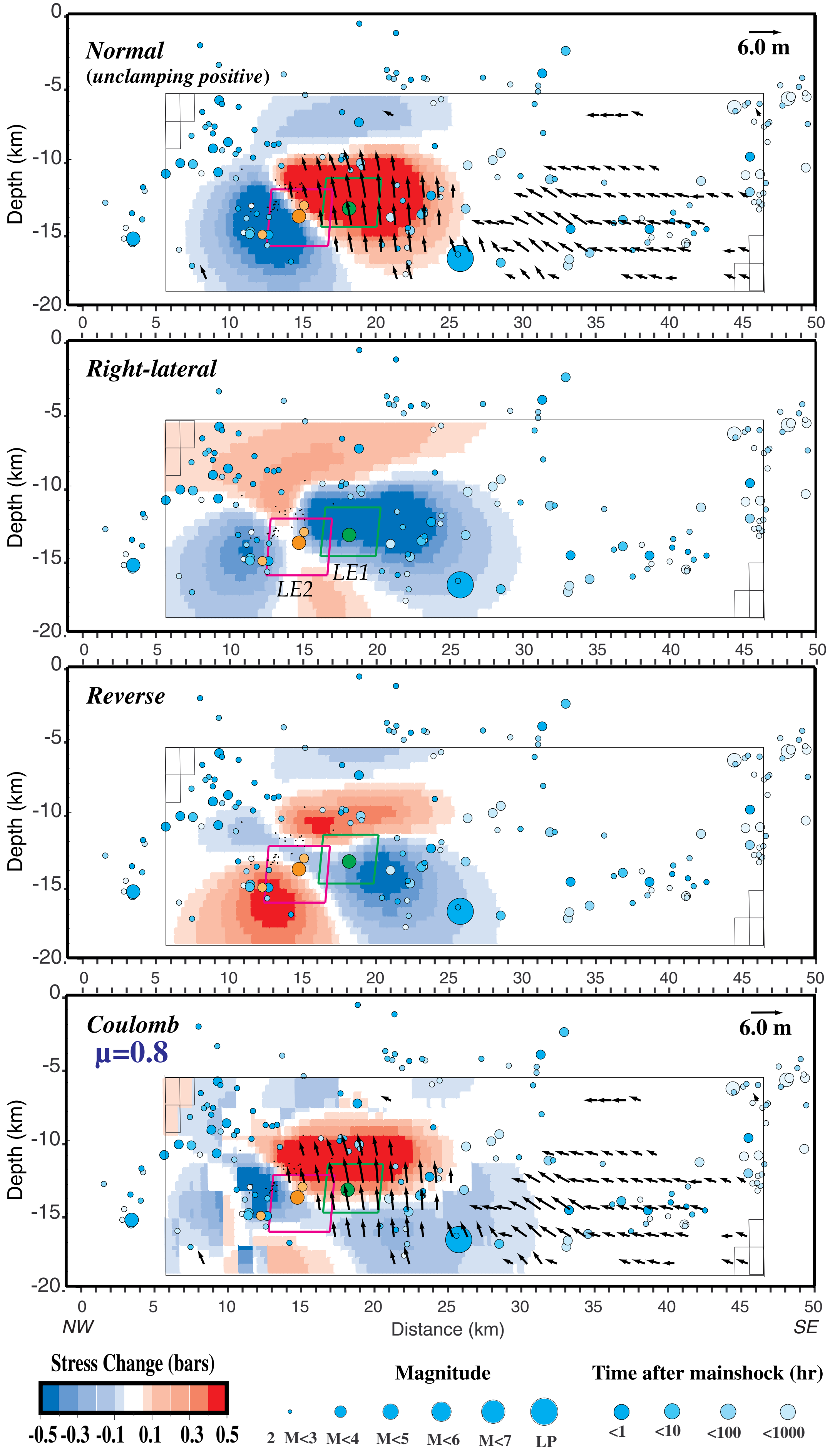
Normal
(unclamping positive)
6.0 m
Right-lateral
LE1
LE2
Reverse
Coulomb
μ=0.8
6.0 m
Depth (km)
0
-5
-10
-15
-20
0
5
10
15
20
25
30
35
40
45
50
NW
Distance (km)
SE
Stress Change (bars)
-0.5 -0.3 -0.1 0.1 0.3 0.5
Magnitude
2 M<3 M<4 M<5 M<6 M<7 LP
Time after mainshock (hr)
<1 <10 <100 <1000

Fig. 4 1 Feb 99

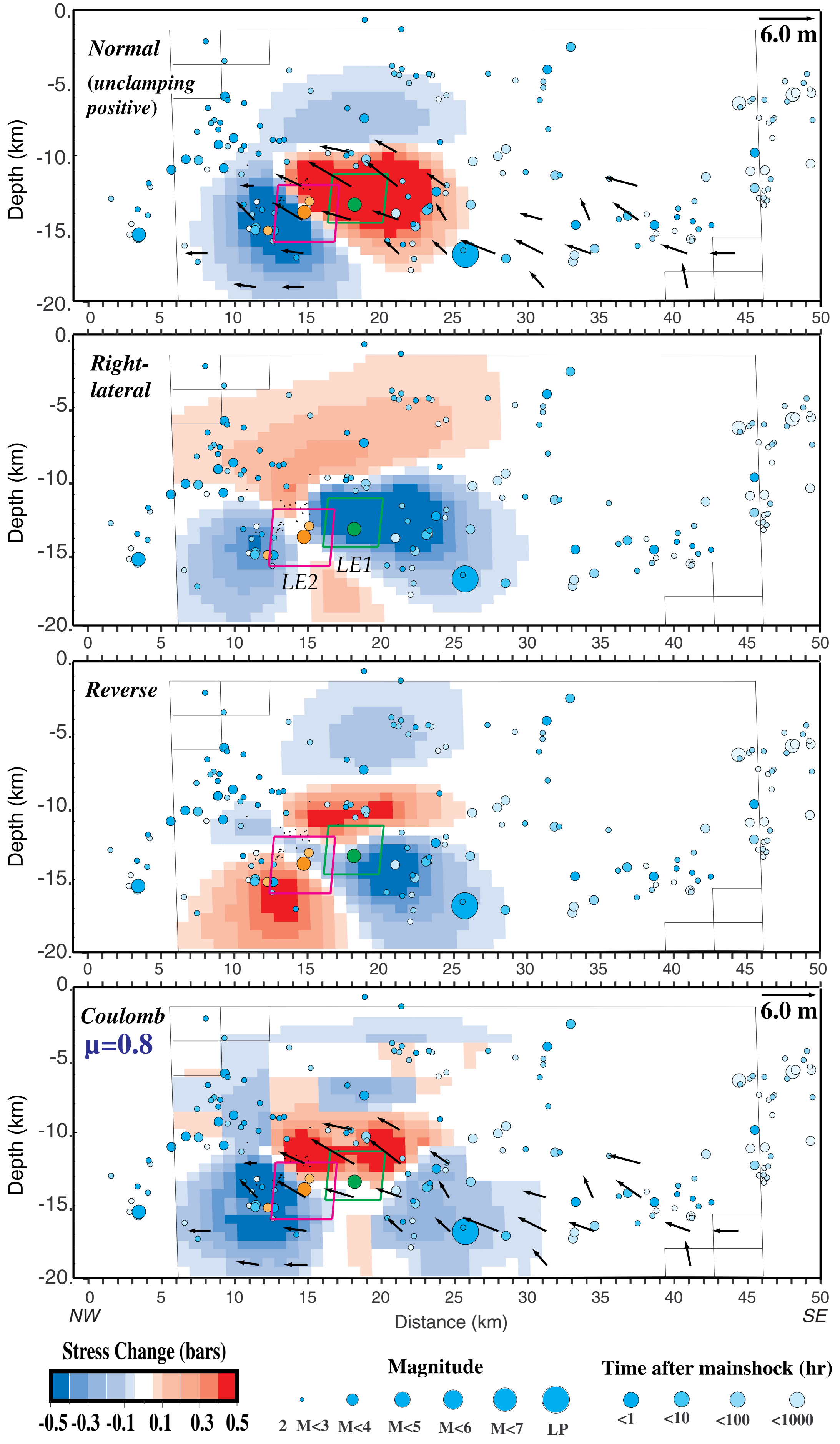
Normal
(unclamping positive)
Right-lateral
Reverse
Coulomb
μ=0.8
6.0 m
LE1
LE2
Depth (km)
0.
-5.
-10.
-15.
-20.
0
5
10
15
20
25
30
35
40
45
50
NW
SE
Distance (km)
Stress Change (bars)
-0.5 -0.3 -0.1 0.1 0.3 0.5
Magnitude
2 M<3
M<4
M<5
M<6
M<7
LP
Time after mainshock (hr)
<1
<10
<100
<1000

Fig. 5   *1 Feb 98*

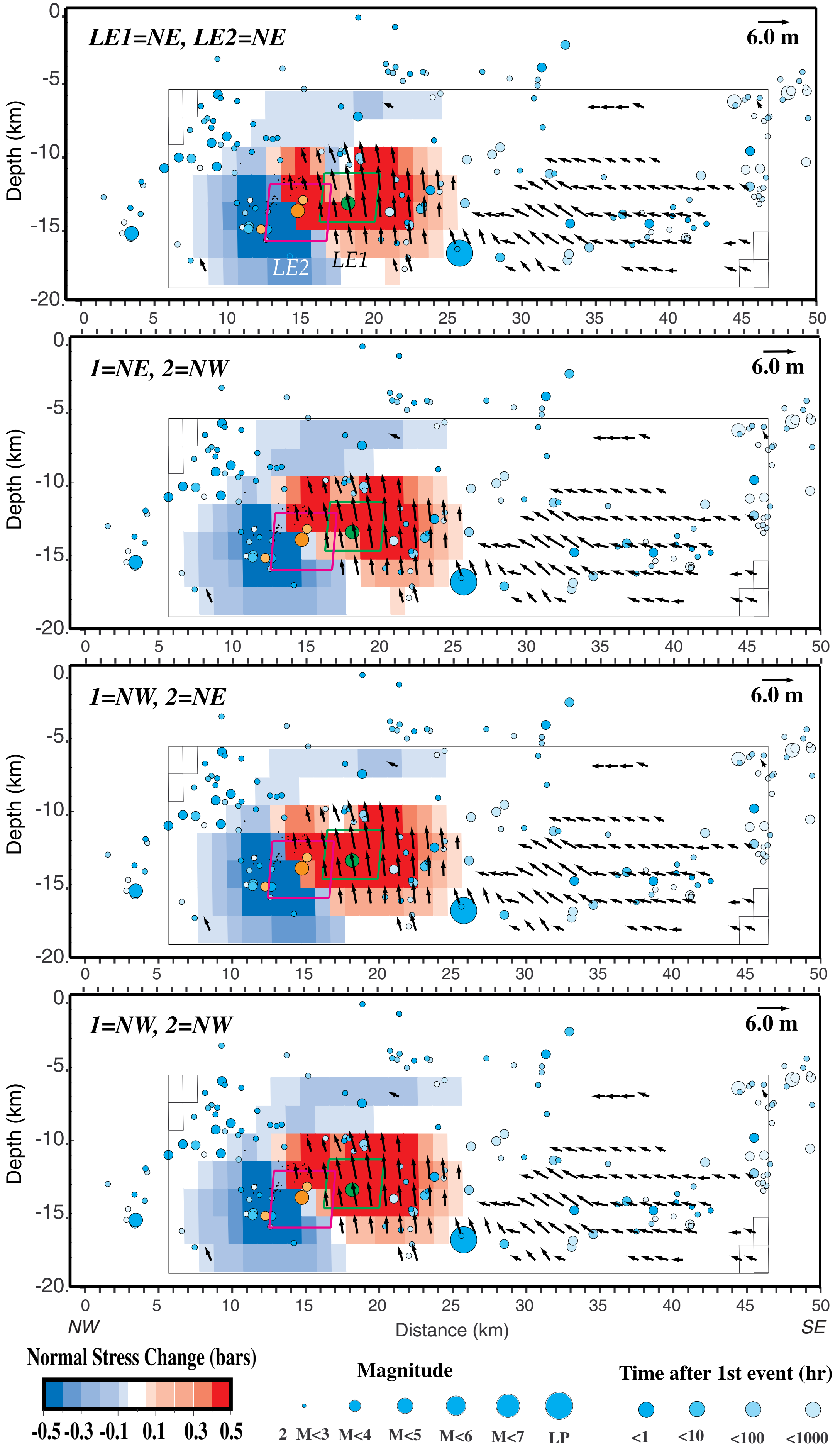
LE1=NE, LE2=NE
1=NE, 2=NW
1=NW, 2=NE
1=NW, 2=NW
6.0 m
LE1
LE2
Depth (km)
0
-5
-10
-15
-20
0
5
10
15
20
25
30
35
40
45
50
NW
SE
Distance (km)
Normal Stress Change (bars)
-0.5
-0.3
-0.1
0.1
0.3
0.5
Magnitude
2
M<3
M<4
M<5
M<6
M<7
LP
Time after 1st event (hr)
<1
<10
<100
<1000

Fig. 6 *1 Feb 98*

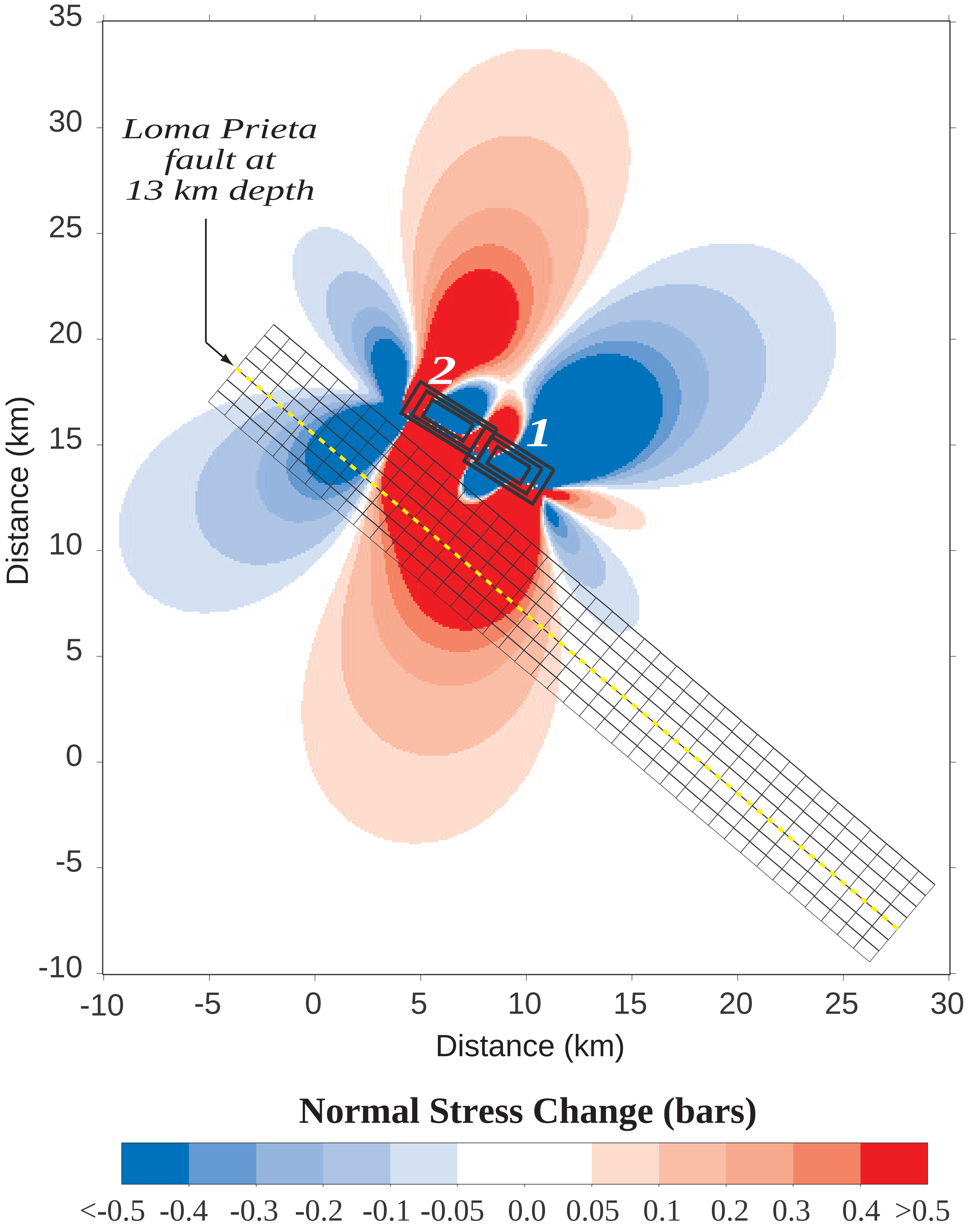

Fig. 7 *30 Jun 98*

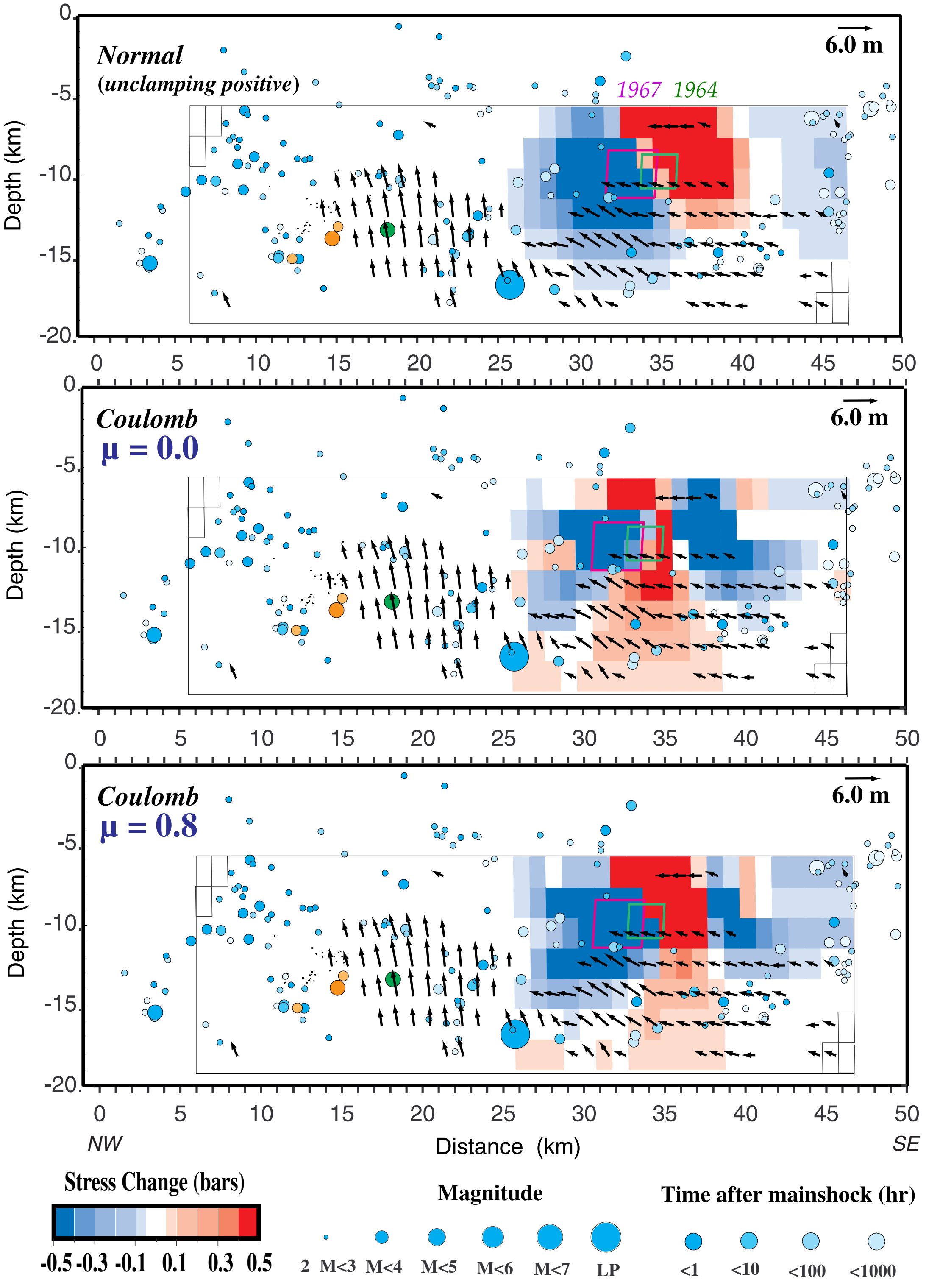
Normal
(unclamping positive)
6.0 m
1967
1964
Depth (km)
0
-5
-10
-15
-20
0
5
10
15
20
25
30
35
40
45
50
Coulomb
μ = 0.0
6.0 m
Coulomb
μ = 0.8
6.0 m
NW
Distance (km)
SE
Stress Change (bars)
-0.5 -0.3 -0.1 0.1 0.3 0.5
Magnitude
2 M<3 M<4 M<5 M<6 M<7 LP
Time after mainshock (hr)
<1 <10 <100 <1000

Fig. 8 1 Feb 99